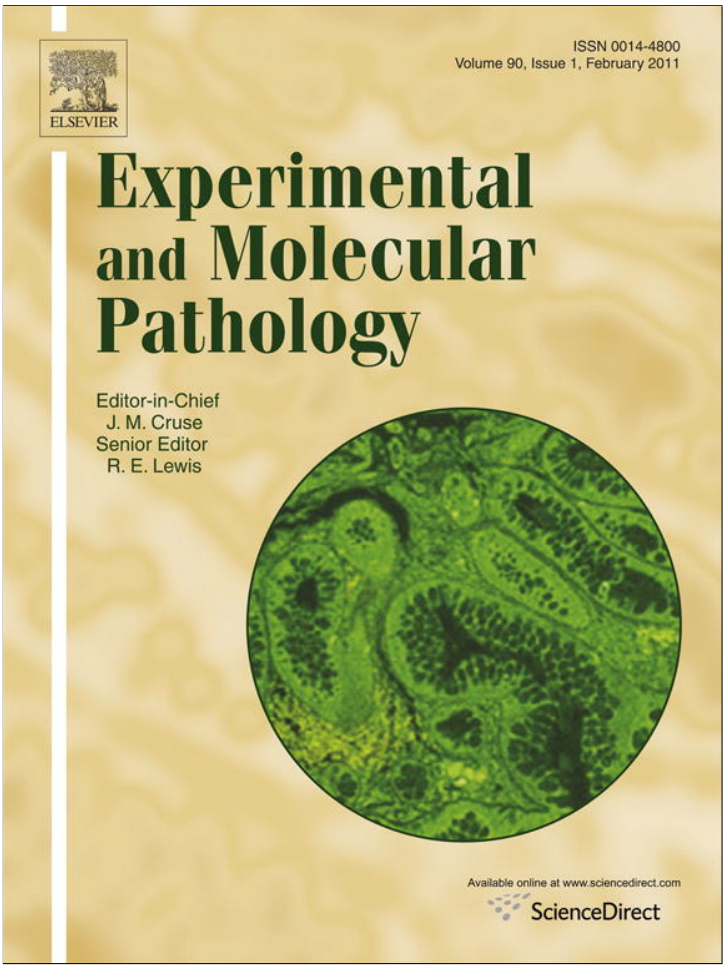

(This is a sample cover image for this issue. The actual cover is not yet available at this time.)

Experimental and Molecular Pathology 91 (2011) 335–345

Contents lists available at ScienceDirect

Experimental and Molecular Pathology

journal homepage: www.elsevier.com/locate/yexmp

C5b-9-activated, $K_v1.3$ channels mediate oligodendrocyte cell cycle activation and dedifferentiation

Cosmin A. Tegla [a,c], Cornelia Cudrici [a], Monika Rozycka [a], Katerina Soloviova [a], Takahiro Ito [a], Anil K. Singh [a], Aamer Khan [a], Philippe Azimzadeh [a], Maria Andrian-Albescu [a], Anver Khan [a], Florin Niculescu [b], Violeta Rus [b], Susan I.V. Judge [a,c], Horea Rus [a,c,d,*]

[a] Department of Neurology, University of Maryland School of Medicine, Baltimore MD, USA
[b] Department of Medicine, Division of Rheumatology and Clinical Immunology, University of Maryland School of Medicine, Baltimore MD, USA
[c] Research Service, Veterans Administration Maryland Health Care System, Baltimore MD, USA
[d] Veterans Administration, Multiple Sclerosis Center of Excellence, Baltimore MD, USA

ARTICLE INFO

Article history:
Received 30 March 2011
Available online xxxx

Keywords:
Voltage-gated potassium channels
Oligodendrocyte
Complement activation
C5b-9
Multiple sclerosis

ABSTRACT

Voltage-gated potassium (K_v) channels play an important role in the regulation of growth factor-induced cell proliferation. We have previously shown that cell cycle activation is induced in oligodendrocytes (OLGs) by complement C5b-9, but the role of K_v channels in these cells had not been investigated. Differentiated OLGs were found to express $K_v1.4$ channels, but little $K_v1.3$. Exposure of OLGs to C5b-9 modulated $K_v1.3$ functional channels and increased protein expression, whereas C5b6 had no effect. Pretreatment with the recombinant scorpion toxin rOsK-1, a highly selective $K_v1.3$ inhibitor, blocked the expression of $K_v1.3$ induced by C5b-9. rOsK-1 inhibited Akt phosphorylation and activation by C5b-9 but had no effect on ERK1 activation. These data strongly suggest a role for $K_v1.3$ in controlling the Akt activation induced by C5b-9. Since Akt plays a major role in C5b-9-induced cell cycle activation, we also investigated the effect of inhibiting $K_v1.3$ channels on DNA synthesis. rOsK-1 significantly inhibited the DNA synthesis induced by C5b-9 in OLG, indicating that $K_v1.3$ plays an important role in the C5b-9-induced cell cycle. In addition, C5b-9-mediated myelin basic protein and proteolipid protein mRNA decay was completely abrogated by inhibition of $K_v1.3$ expression. In the brains of multiple sclerosis patients, C5b-9 co-localized with $NG2^+$ OLG progenitor cells that expressed $K_v1.3$ channels. Taken together, these data suggest that $K_v1.3$ channels play an important role in controlling C5b-9-induced cell cycle activation and OLG dedifferentiation, both in vitro and in vivo.

Introduction

Oligodendrocytes (OLGs) myelinate the axons of the central nervous system (CNS) and undergo apoptosis during development (Tang et al., 2001; Trapp et al., 1997). In the developing CNS, OLGs are selectively rescued from apoptosis by survival signals provided by axonal contact and growth factors (Barres and Raff, 1999; Billon et al., 2002). A correlation has been demonstrated between the expression of the delayed, outward-rectifying voltage-gated K_v channels and the proliferative potential of OLG-lineage cells. Proliferating OLG progenitor cells (OPCs) display large K_v currents, whereas postmitotic OLGs do not express such currents (Attali et al., 1997; Chittajallu et al., 2002). However, few studies have attempted to identify the cellular mechanisms responsible for these K_v channel changes in OPCs and mature OLGs (Vautier et al., 2004). Several K_v1 (KCNA) family members ($K_v1.1$–1.6) have been described in immature OLGs on both the mRNA and protein levels. Significant levels of $K_v1.2$, $K_v1.3$, $K_v1.4$, $K_v1.5$, and $K_v1.6$ have been found, with $K_v1.3$ and $K_v1.5$ being up-regulated under the influence of proliferation-stimulating growth factors (Attali et al., 1997; Chittajallu et al., 2002). $K_v1.3$ is the main KCNA family member involved in the regulation of proliferation and differentiation of oligodendroglial cells (Attali et al., 1997; Chittajallu et al., 2002). Currents passing through $K_v1.3$-containing channels play an important role in the G_1/S transition of proliferating OPCs. Inhibition of K_v channels also causes an accumulation of the cyclin-dependent kinase inhibitors p27 and p21 as well as G1 arrest in OPCs (Ghiani et al., 1999). In addition, K_v channel blockage has been shown to impair remyelination in a cuprizone model of demyelination (Bacia et al., 2004).

Complement activation and the subsequent assembly of the terminal complement complex (C5b-9, composed of the C5b, C6, C7, C8, and C9 proteins) play a significant role in the pathogenesis of a variety of CNS diseases, including multiple sclerosis (MS; reviewed in (Rus et al., 2006)). By forming pores in the plasma membrane, C5b-9 causes cell death and induces apoptosis (Cragg et al., 2000;

* Corresponding author at: University of Maryland, School of Medicine, Department of Neurology, 655 W Baltimore St, BRB 12-033, Baltimore, MD 21201, USA. Fax: +1 410 706 0186.
E-mail address: hrus@umaryland.edu (H. Rus).

0014-4800/$ – see front matter © 2011 Elsevier Inc. All rights reserved.
doi:10.1016/j.yexmp.2011.04.006

Papadimitriou et al., 1994, 1991). However, like other nucleated cells, OLGs can survive limited C5b-9 complement attack through the protection provided by complement-inhibitory proteins and by the elimination of membranes carrying C5b-9 complexes (Carney et al., 1985; Scolding et al., 1989). We have shown that C5b-9 at sublytic doses inhibits the mitochondrial pathway of apoptosis (Soane et al., 2001, 1999) and Fas-mediated apoptosis by regulating caspase-8 processing (Cudrici et al., 2006). C5b-9 activates the cell cycle in OLGs (Rus et al., 1997, 1996), and this induction of the S phase of the cell cycle is c-Jun-dependent (Rus et al., 1996). These C5b-9 pro-survival effects are mediated by the activation of the ERK1 and phosphatidylinositol 3-kinase (PI3K)/Akt pathways, a process that is Gi protein-dependent (Rus et al., 1997, 1996; Soane et al., 2001).

To date, the role of inflammation in modulating $K_v1.3$ expression by OLGs during demyelination has not been evaluated. Complement activation and C5b-9 deposition are hallmarks of the most frequently pathological form of MS, the type II pattern (Lucchinetti et al., 2000). However, it is not clear at present whether K_v channels are involved in the OLG cell cycle activation mediated by C5b-9 or how K_v channel expression might affect the signaling pathways involved in cell activation.

In the present report, we have demonstrated that $K_v1.3$ is involved in the cell cycle activation induced by C5b-9. Since both the ERK and Akt pathways are known to be induced by C5b-9, we assessed the possible role of $K_v1.3$ in the activation of these kinases. Inhibition of $K_v1.3$ by rOsK-1 significantly reduced Akt phosphorylation and activation by C5b-9 but had no effect on ERK1 activation. In addition, we found that C5b-9-mediated myelin basic protein (MBP) and proteolipid protein (PLP) mRNA down-regulation was completely abrogated by inhibition of $K_v1.3$ expression. In the brains of patients with MS, C5b-9 was co-localized with $NG2^+$ cells that expressed $K_v1.3$ channels. In conclusion, our data suggest that $K_v1.3$ channels play an important role in controlling cell cycle activation by affecting the C5b-9-mediated activation of Akt and may also have a significant role in OLG dedifferentiation.

Material and methods

Brain tissue

Frozen brain tissue specimens were obtained at autopsy from 6 patients with a definitive diagnosis of MS from the Human Brain and Spinal Fluid Resource Center, Veterans Affairs West Los Angeles Health Care Center. Active lesions contained abundant infiltrates consisting of T cells and macrophages with detectable myelin degradation products. Inflammation was restricted to the lesion margins in chronic active lesions. Regions of normal appearing white matter (NAWM) and normal appearing gray matter lesions (NAGM) that lacked macroscopic or histological evidence of demyelination were also used. The samples were derived from patients between the ages of 30 and 62 with a mean age of 50. Four healthy control samples were obtained from Cooperative Human Tissue Network, Charlottesville, VA.

Primary cultures of OLG progenitor cells and OLGs

Neonatal OLGs were purified from the brains of 1-day-old Sprague–Dawley rats as previously described (Soane et al., 2001). After removal of the meninges, the brain was minced and sequentially passed through nylon meshes. The dissociated cell suspension was plated onto 75-cm^2 plates in DMEM/Ham's F-12 medium containing 10% fetal serum bovine (FBS). OPCs were separated from the astrocyte monolayer by shaking overnight at 200 rpm on a rotary shaker. The OPC cell suspension was collected and resuspended in defined medium containing serum-free DMEM/Ham's F-12, transferrin (500 ng/ml; Sigma Chemical Co., St. Louis, MO), insulin (75 ng/ml; Sigma), bFGF (75 μg/ml; Peprotech Inc, Rocky Hill, NJ) and 1 mM sodium pyruvate (Sigma). The cells were differentiated at 37 °C for 52 h. Over 85% of the cells expressed myelin basic protein (MBP), proteolipid protein (PLP), and galactocerebroside (GC). Fewer than 3% of the cells were negative for MBP and were astrocytes or OPC in varying stages of differentiation.

Membrane assembly of sublytic C5b-9 using terminal complement proteins

Purified human complement proteins C5b6, C7, C8, and C9 were obtained from Quidel (San Diego, CA) and Advanced Research Technologies (San Diego, CA). In brief, OLGs were incubated at 37 °C with 18 U of C5b6 and 10 μg/ml each of C7, C8, and C9 in a final volume of 2 ml for the indicated periods of time. In some experiments, normal human serum (NHS) pooled from several healthy donors was used as a source of serum complement. Rabbit antiserum recognizing GC was used to sensitize rat OLG; the cells were then incubated with NHS, heat-inactivated NHS (HI-NHS) or NHS containing K76 COONa (Otsuka Pharmaceuticals Co, Tokyo, Japan) at a final dilution of 1/10 for various time periods. As previously described, K76 prevents C5b-9 assembly in serum by binding to C5 (Niculescu et al., 1997; Rus et al., 1996). The concentrations of complement proteins used in this study were sublytic for OLG, as determined by staining cells with the vital dye trypan blue and measuring release of cytoplasmic lactate dehydrogenase as an indicator of cell death (Niculescu et al., 1997).

Electrophysiological studies

Cells were voltage-clamped using the whole-cell variation patch-clamp technique as previously described. Data acquisition and analysis was performed using an AxoPatch 200B patch clamp amplifier, Digidata 1332A analog-to-digital converter, and pClamp 8.2 software (Molecular Devices Corp., Sunnyvale, CA). Pipettes with a tip resistance of 2 to 3 MΩ were made from borosilicate glass (World Precision Instruments, New Haven, CT) on a micropipette puller (Model P-2000; Sutter Instrument Company, Novato, CA) and heat-polished. The pipette was filled with a previously filtered solution composed of (in mMol/l): 2 $NaCl_2$, 145 KCl, 1 $MgCl_2$, 5 EGTA, and 10 HEPES (the pH was adjusted to 7.3 with potassium hydroxide). The standard bath solution contained (in mMol/l): 135 NaCl, 5 KCl, 2 $CaCl_2$, 1 $MgCl_2$, and 10 HEPES (pH adjusted to 7.4 with NaOH). The osmolarity of the solutions was adjusted with D-glucose to 300 and 305 mOsm, respectively. Currents were low-pass-filtered at 2 or 5 kHz and sampled at 5 or 10 kHz. Data analysis was performed using Clampfit (version 8.2 of pClamp) and SigmaPlot 8.0 (SYSTAT Software, Point Richmond, CA). The pipette offset current was zeroed immediately before contacting the cell membrane. Only standard whole-cell experiments with access resistance <10 MΩ and membrane resistance >400 MΩ were included in this study. The membrane capacitances of the analyzed cells varied between 10 and 40 pF. Linear capacitance and leakage currents were subtracted online using a standard P/4 protocol. K_v currents were elicited by 500-ms pulses stepped from a holding potential of −60 to +60 mV, preceded by a conditioning pulse of −110 mV for 200 ms. Resting potential V_R (zero-current potential) was determined from current–voltage recordings, measured during the first few minutes after achieving the whole-cell recording conformation. The threshold for activation V_A was estimated from voltage–current relationship. After the whole-cell configuration was established and control measurements were made, serum C5b-9 was added directly to the experimental chamber. After 5–8 min of incubation, the measurements were repeated. The time of incubation was established in separate experiments on 10 cells (data not shown). Because of the cell-to cell variability, the evaluation of the effect of C5b-9 on the outward currents in OLGs was done for each cell independently. Statistical analysis comparing the chord conductance for control cells and that treated for cells with serum C5b-9 was performed using t-tests for paired observations. The statistical significance of an

observed shift in half-maximal activation $V_{1/2}$ value between the control and treated cells was assessed with the Wilcoxon matched-pairs signed-rank test at a significance level of $\alpha = 0.01$.

To examine the effect of rOsK-1 on the outward current in OLGs pretreated with C5b-9, we performed electrophysiological measurements on 15 cells. rOsK-1 at a final concentration of 5 nM was added directly to the experimental chamber, following the recordings performed consecutively on the non-treated and C5b-9 treated cells. The chord relative conductance values, measured at $V_h = 60$ mV, were then compared between experimental groups.

Western blot analysis

Western blotting was performed as previously described (Rus et al., 1996). OLGs were washed with PBS, then lysed in a buffer consisting of 10 mM Tris–HCl (pH 7.4), 1 mM EDTA, 1 mM EGTA, 1 mM NaF, 20 mM $Na_4P_2O_7$, 1% Triton X-100, 0.1% SDS, 100 mM NaCl, 10% glycerol, 0.5% sodium deoxycholate, 1 mM Na_3VO_4, and complete mini protease inhibitor mixture (Roche Applied Science, Indianapolis, IN), which was added just prior to use. Protein concentrations were determined using a BCA protein assay kit (Pierce, Rockford, IL). Samples were fractionated on an SDS-polyacrylamide gel and transferred to a nitrocellulose membrane (Millipore, Bedford, MA). The membrane was blocked with 0.1%Tween-TBS containing 1% bovine serum albumin (BSA) for 1 h and incubated with primary antibody overnight at 4 °C. Goat anti-rabbit or anti-mouse IgG-HRP conjugated antibodies (Santa Cruz Biotech) were applied for 1 h at room temperature. After washing, the immune complexes were detected using enhanced chemiluminescence (Pierce). The primary antibodies used for western blotting (all rabbit IgG) were: anti-K_v1.3 (Alomone Labs and Chemicon), anti-phospho-ERK1 (Cell Signaling), anti-ERK1 (Santa Cruz Biotech), anti-FOXO1 and pFOXO1 (Cell Signaling), anti-Akt and pAkt (Ser 473) (Santa Cruz Biotech). Membranes were stripped using Restore Western Blot Stripping Buffer (Pierce) and reprobed for the expression of β-actin (Rockland Immunochemicals, Rockville, MD). The radiographic band density was measured using UN-SCAN-IT software (Silk Scientific, Orem, UT), and the results were expressed as ratios of the density to the density of β-actin. All experiments were performed in triplicates.

Real-time PCR

Total RNA obtained was purified using the RNeasy Mini Kit (Qiagen, Santa Clarita, CA) according to the manufacturer's instructions. RNA (0.5 μg per sample) was mixed with RT buffer, dNTP, and oligo-dT primer (Invitrogen). RNA was denatured by incubation at 65 °C for 5 min. The reverse transcriptase (Promega) and RNase inhibitor (Invitrogen) were then added, and the reaction mixture was incubated at 37 °C for 1 h. The reaction was terminated by incubation of the mixture at 95 °C for 5 min.

Real-time PCR was performed using a StepOne real-time PCR system (Applied Biosystems, Foster City, CA). The primers for the genes investigated were designed and synthesized by TIB Mol Biol LLC (Adelphia, NJ) (Table 1) and used in conjunction with FastStart SYBR Green Master (Roche) according to the manufacturer's protocol. As a negative control for each real-time PCR assay, the same reaction was performed in the absence of cDNA or reverse transcriptase. For each gene, the cycle threshold (C_T) values were determined in the exponential phase of the amplification plot and normalized by subtraction of the C_T value for 18S (generating a ΔC_T value). The -fold change in target gene samples, after normalization with the housekeeping gene (18S), was calculated using the $2^{-\Delta\Delta CT}$ value, where $\Delta\Delta C_T = \Delta C_T$ (sample) $- \Delta C_T$ (control) and ΔCT is the C_T value of target gene normalized to the C_T value of the housekeeping gene (Cudrici et al., 2008).

Table 1
Primers used for Real-Time PCR.

Gene symbol	Primers sequence	Product (bp)
Kv1.3 (KCNA3)	For: 5′-ACACAGCTCAAGACCCTCTG-3′ Rev: 5′-TTGGTAGAAGCGGATCTCCT-3′	216
MBP	For: 5′-GCTGGGGAGGAAGAGACAG-3′ Rev: 5′-CCACGGGATTAAGAGAGGGT-3′	170
PLP	For: 5′-CCACCTGTTTATTGCTGCAT-3′ Rev: 5′-TGTGGTTAGAGCCTCGCTATT-3′	171
18S	For: 5′-GTAACCCGTTGAACCCCATT-3′ Rev: 5′-CCATCCAATCGGTAGTAGCG-3′	151

For, forward primer; Rev, reverse primer; Bp, base pairs; KCNA3, potassium voltage-gated channel, shaker-related subfamily, member 3; MBP, myelin basic protein; PLP1, proteolipid protein 1; 18S, 18S ribosomal RNA.

DNA synthesis

DNA synthesis testing was performed as previously described (Fosbrink et al., 2009; Niculescu et al., 1997). In some cases cultured cells were pretreated with 4-aminopyridine (4AP, 5 mM) or rOsK-1 (Alomone Lab, Jerusalem, Israel) (5 nM and 15 nM) prior to stimulation with C5b-9. After stimulation, 1 μCi/ml of [^{3}H]thymidine (Perkin Elmer, Boston MA) was added to the cells. The plate was incubated at 37 °C with 5% CO_2 for 18 h. The cells were lysed and precipitated by adding 20% trichloroacetic acid, and the precipitated DNA was filtered through Whatman GF/A filter paper (Whatman, Maidstone, UK). The filter paper was air-dried, and the radioactivity was counted by liquid scintillation.

Immunohistochemical staining for NG2, K_v1.3, and C5b-9

Immunohistochemical staining of brains from MS patients was performed as previously described (Cudrici et al., 2005). The air-dried cryostat sections (4–6 μm) were fixed for 10 min in acetone containing 0.3% H_2O_2 to remove endogenous peroxidase. Sections were blocked for 10 min with horse serum, then incubated overnight at 4 °C with mouse monoclonal antibody against NG2 (clone 9.2.27, BD Pharmingen, San Jose, CA). The sections were washed three times for 3 min each with PBS, pH 7.4, and incubated for 30 min with biotinylated "universal" secondary antibody (Vector, Burlingame, CA), then for 30 min at room temperature with the Vectastain RTU ABC Reagent. The specific reaction was developed using NovaRED (Vector Labs, Burlingame, CA). For K_v1.3 and C5b-9 detection, cryosections were processed as described above and then incubated at 4 °C overnight with rabbit IgG anti-Kv1.3 (Chemicon) diluted 1/100 or rabbit IgG anti-C5b-9 neoantigens (Dako, Carpanteria, CA) diluted 1/50. The sections were washed with PBS, pH 7.4, and then incubated for 1 h at room temperature with HRP-conjugated goat anti-rabbit IgG (Santa Cruz Biotech, Santa Cruz, CA). The specific reactions were developed using NovaRED (Vector Labs, Burlingame, CA).

Double immunohistochemical staining

Frozen sections of brains from adult patients with MS were double-stained for NG2 and C5b-9 and for NG2 and K_v1.3. Cryosections were initially processed for NG2 immunostaining as described above, and the reaction developed with NovaRed. The sections were then treated with 0.3% H_2O_2 to remove excess peroxidase and incubated overnight at 4 °C with rabbit anti-C5b-9 diluted 1/50 or with anti-K_v1.3 diluted 1/100. The slides were washed several times in PBS, reacted with HRP-conjugated goat anti-rabbit antibody (Jackson Immunoresearch Labs) and exposed to diaminobenzidine (Pierce, Rockford, IL) or with alkaline phosphatase (AP)-conjugated goat anti-rabbit and then exposed to Vector Blue AP substrate III (Vector Labs). Control sections were prepared by immunostaining without the primary antibody or by using control isotype IgG instead

of the primary antibody. The immunostained slides were independently evaluated by two investigators.

Results

Decreased expression of $K_v1.3$ during OPC differentiation

Our real-time PCR analysis revealed that OPC differentiation was associated with a significant increase in the expression of MBP and PLP mRNA (Fig. 1A). High levels of $K_v1.3$ expression were found in the OPCs. However, the expression of $K_v1.3$ mRNA was significantly decreased at 56 h of OLG differentiation ($p=0.021$) when compared to OPC levels (Fig. 1B). We then asked whether similar changes occurred in $K_v1.3$ protein expression. Our data showed that the initially high levels of $K_v1.3$ protein seen in OPCs decreased significantly during the course of differentiation (Fig. 1C). After 48 h of differentiation, the expression of $K_v1.3$ was reduced by 75% ($p=0.029$) (Fig. 1C). $K_v1.4$ protein levels were found to be high in OPCs, and the levels remained unchanged during differentiation (Fig. 1C).

Effect of sublytic C5b-9 on $K_v1.3$ protein expression in OLGs

Given the alteration in $K_v1.3$ protein expression that we observed during differentiation, we decided to concentrate our further efforts on investigating the effect of sublytic concentrations of C5b-9 on $K_v1.3$ expression. We first asked whether C5b-9 had the ability to affect the protein expression of $K_v1.3$. When we cultured OLGs in defined medium in the presence of C5b-9 or C5D, we found that sublytic concentrations of C5b-9 induced a significant increase of $K_v1.3$ expression when compared to C5D ($p=0.05$) (Fig. 2A). Pretreatment with rOsK-1 (Alomone Labs, Jerusalem, Israel), a $K_v1.3$ inhibitor, significantly reduced this effect ($p=0.007$) (Fig. 2B). The effect of rOsK-1 was similar at 5 and 15 nM (data not shown). The effect on $K_v1.3$ expression was detectable after 15 min of exposure to C5b-9 and persisted for more than 2 h (data not shown). In contrast, exposure to C5b6 or C5D had no significant effect on $K_v1.3$ expression (Fig. 2A). Similar results were obtained using two different anti-$K_v1.3$ antibodies (data not shown). The increase in $K_v1.3$ protein expression was most probably the result of an increase in the half-life at the plasma membrane, since the mean half-life of the $K_v1.3$ increased by 1.6 times in the C5b-9 stimulated OLGs in the presence of cycloheximide (10 μg/ml) (data not shown). A similar increase in the half-life of the $K_v1.3$ protein was reported in TrkB-induced up-regulation of this channel's expression (Colley et al., 2007).

Effect of sublytic C5b-9 on the total membrane outward current in OLGs

In order to determine whether this increase in $K_v1.3$ expression was associated with the presence of a functional channel, we measured the amplitude and kinetic properties of the total recorded current. The values obtained for control (untreated) cells were in agreement with those obtained previously, showing characteristic

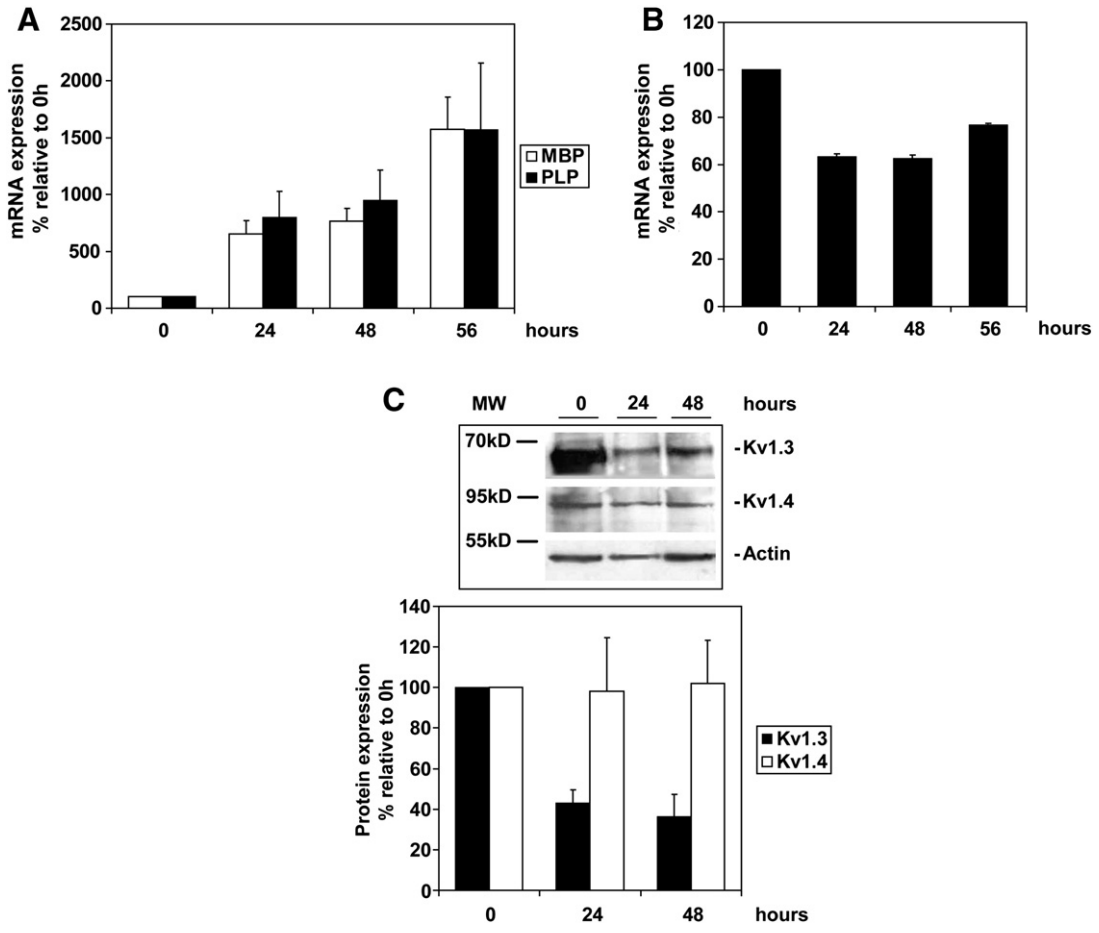

Fig. 1. MBP, PLP, and $K_v1.3$ mRNA expression during OLG differentiation. OPCs were cultured in defined medium for the indicated times, and the expression of $K_v1.3$, K_v 1.4, MBP, and PLP mRNA was determined. A. Expression of MBP and PLP mRNA, as determined by real-time PCR, significantly increased during OLG differentiation. B. $K_v1.3$ mRNA was present in the OPC cells (0 h), and the levels decreased significantly at 48 h of differentiation ($p=0.0007$). C. The effect of differentiation on K_v protein expression was examined by western blotting and expressed as a ratio to β-actin. High levels of $K_v1.3$ protein were found in OPCs, and these levels decreased significantly during differentiation ($p=0.029$). The levels of $K_v1.4$ did not change significantly during differentiation. The expression of the mRNA or protein at the beginning of the experiment (0 h) was considered to be 100%. Results of three separate experiments are expressed as mean ± SEM, relative to the value at 0 h.

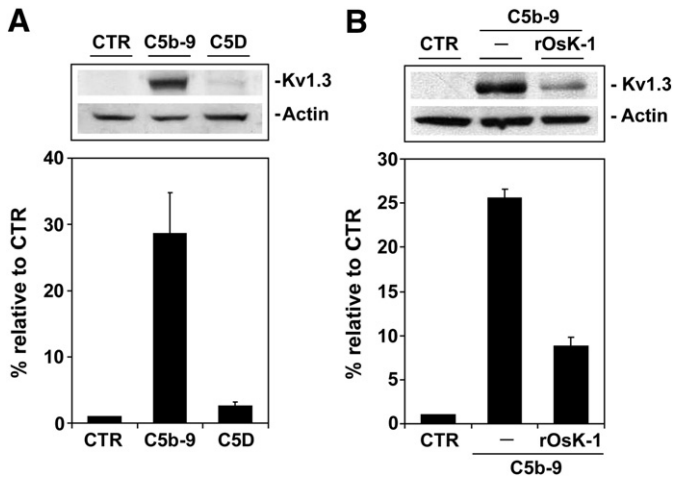

Fig. 2. Effect of C5b-9 on $K_v1.3$ expression in OLGs. A. C5b-9 induces $K_v1.3$ expression. OLGs were cultured in defined medium and exposed to C5b-9 or C5D, and $K_v1.3$ expression was determined by western blotting. $K_v1.3$ protein expression was found to be low in the differentiated OLGs (CTR) and was significantly increased after exposure to C5b-9 ($p=0.042$). C5D serum had no significant effect on $K_v1.3$ expression, indicating that the increase seen was dependent on the assembly of the terminal pathway. The results are expressed as means ± SEM. Data are derived from three separate experiments. B. rOsK-1 inhibits $K_v1.3$ expression induced by C5b-9. OLGs were pretreated with rOsk-1 (15 nM) for 1 h and then exposed to C5b-9 for 30 min. Lysates were analyzed by western blotting for $K_v1.3$ and β-actin expression. Exposure to rOsk-1 was able to reverse the effect of C5b-9 on $K_v1.3$ expression ($p=0.007$), indicating that channel expression is required for the C5b-9 effect.Results of three separate experiments are expressed as mean ± SEM, relative to the control (CTR).

cell-to-cell variability (Attali et al., 1997; Chittajallu et al., 2002; Soliven et al., 1989; Vautier et al., 2004). In the majority of the cells, the dominant currents were slow or non-inactivating. In seven cells, the fast and moderately inactivating current components were predominant in the total outward current, indicating strong expression of $K_v1.3$ in those cells (data not shown). After establishing the whole-cell configuration and obtaining control measurements, we added C5b-9 directly to the experimental chamber. After 5–8 min of incubation, the measurements were repeated. Because of the cell-to-cell variability, the effect of C5b-9 on the outward currents in OLGs was evaluated independently for each cell. Current recordings from 22 cells were analyzed. In 19 of the 22 studied cells, we observed a significant increase ($p<0.01$) in current conductance after exposure to C5b-9 (Supplemental Fig. 1A). This increase in current conductance was accompanied by a significant ($p<0.01$) shift in the half-maximal activation $V_{1/2}$ values in a more positive direction. In most cases, the chord conductance increased by 10–50% (median, 35%, Supplemental Figs. 1B,C). Overall, these observations suggest that sublytic C5b-9 increased the number of functioning K_v channels, with the cell-to-cell variations in whole-cell macroscopic currents likely reflecting composites of several members of the K_v1 subfamily.

We then used rOsK-1 to investigate the role of $K_v1.3$ in the current changes induced by C5b-9, which was added directly to the experimental chamber, after consecutive recordings had been obtained for untreated (control) and C5b-9-treated cells (Figs. 3A,B,C). The concentration used (5 nM) used produced nearly complete inhibition of the $K_v1.3$ channels present in the cell's membrane. The chord relative conductance values, measured at $V_h=60$ mV, were then compared between experimental groups. In 7 of the 15 rOsK-1-treated cells, the inhibitor had no effect on the electrophysiological characteristics of the total outward currents. In the case of five cells, the conductance measured for the rOsK-1-treated cell was lower than that for the control or C5b-9 treated cell (Fig. 3D). In three cells, the relative conductance measured for rOsK-1-treated cells was lower than that calculated for serum C5b-9-treated cells, yet the value remained higher than that for control cells. Point-by-point subtraction of the current traces obtained after application of rOsK-1 from the traces generated by C5b-9 revealed the current blocked by the application of 5 nM rOsK-1 to be moderately inactivating and $K_v1.3$-like (Fig. 3E). These data indicated that exposure to C5b-9 altered the

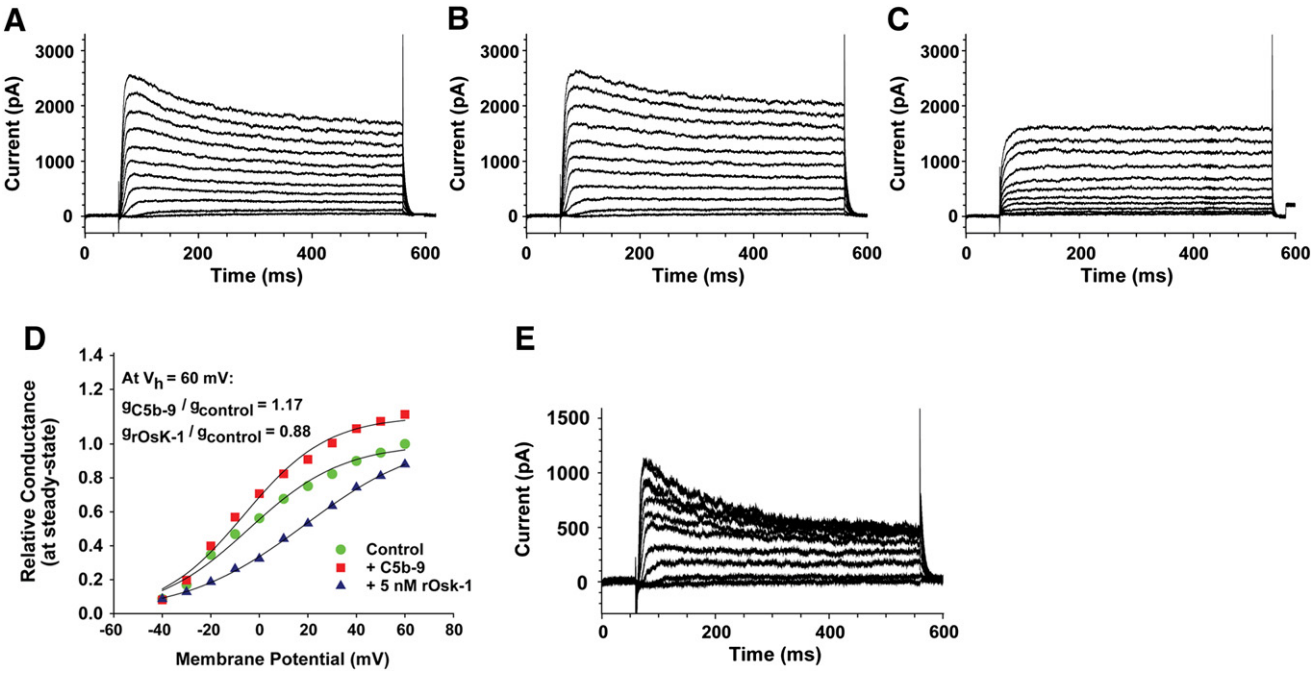

Fig. 3. Effect of rOsk-1 on C5b-9 induced outward currents in OLGs. K_v currents were elicited by 500-ms pulses stepped from a holding potential of −60 to +60 mV, preceded by a conditioning pulse of −110 mV for 200 ms. C5b-9 was added directly to the experimental chamber. After 5–8 min of incubation, the measurements were repeated, then 5 nM rOsK-1 5 nM final concentration was added to the experimental chamber and measurements were repeated. A–C. Examples of whole-cell current families derived from an unstimulated cell (A), the same cell stimulated with C5b-9 (B) and treated with 5 nM rOsK-1 (C). D. Relative membrane conductance as a function of membrane potential for control (unstimulated) cell (dots), after stimulation with C5b-9 (squares) and after treatment with 5 nM rOsK-1 (triangles). E. Example of the current elicited by C5b-9 and blocked by rOsK-1. Point-by-point subtraction of the current traces obtained after application of rOsK-1, from the current traces evoked by C5b-9 revealed a moderately inactivating, $K_v1.3$-like current.

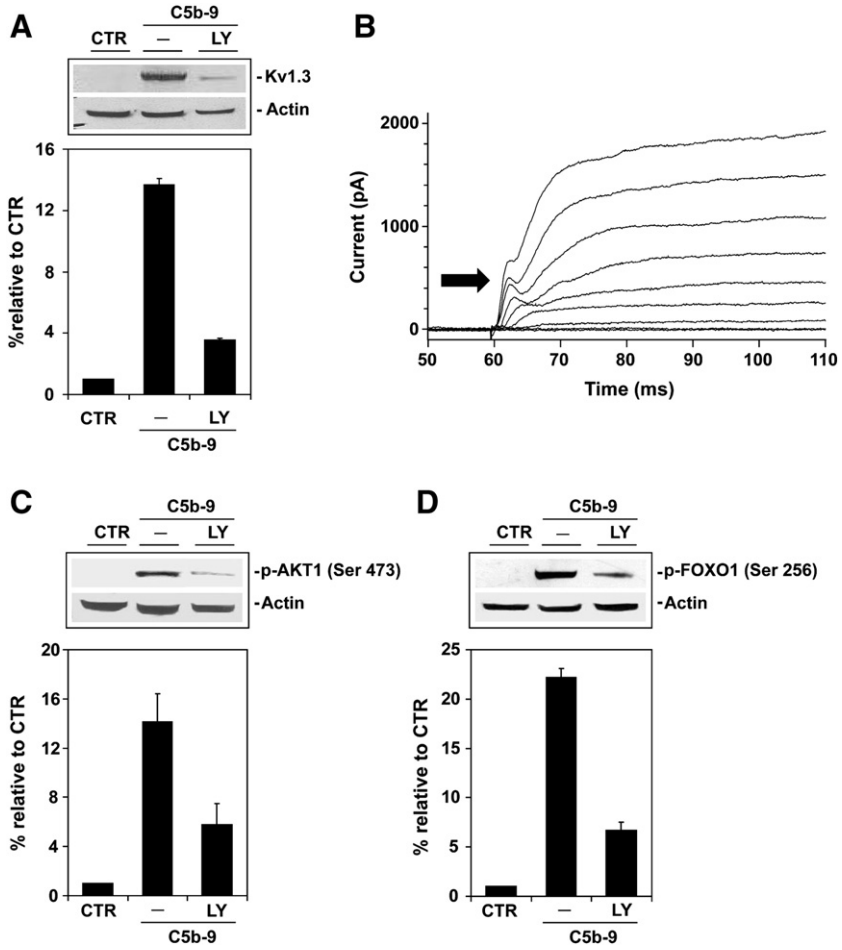

Fig. 4. The effect LY294002 on C5b-9-induced $K_v1.3$ and outward current. A. OLGs were pretreated with the PI3K inhibitor LY294002 (10 or 20 μM) for 1 h, then exposed to C5b-9 for 30 min. Lysates were analyzed by western blotting for $K_v1.3$ as described above. Exposure to LY294002 (20 μM) was able to reverse the effect of C5b-9 on $K_v1.3$ ($p = 0.016$). B. Point-by-point subtraction of the current traces elicited from the C5b-9-stimulated cells obtained prior to and after application of LY294002 (20 μM) revealed the whole-cell currents blocked by LY294002. The electrophysiological measurements were performed in 10 cells. C, D. OLGs were pretreated with the PI3K inhibitor LY294002 (10 or 20 μM) for 1 h, then exposed to C5b-9 for 30 min. Lysates were analyzed by western blotting for Akt and FOXO1 as described above. Exposure to LY294002 was able to reverse the effect of C5b-9 on Akt (C) and FOXO1 phosphorylation (D). Results of three separate experiments are expressed as mean ± SEM, relative to the CTR.

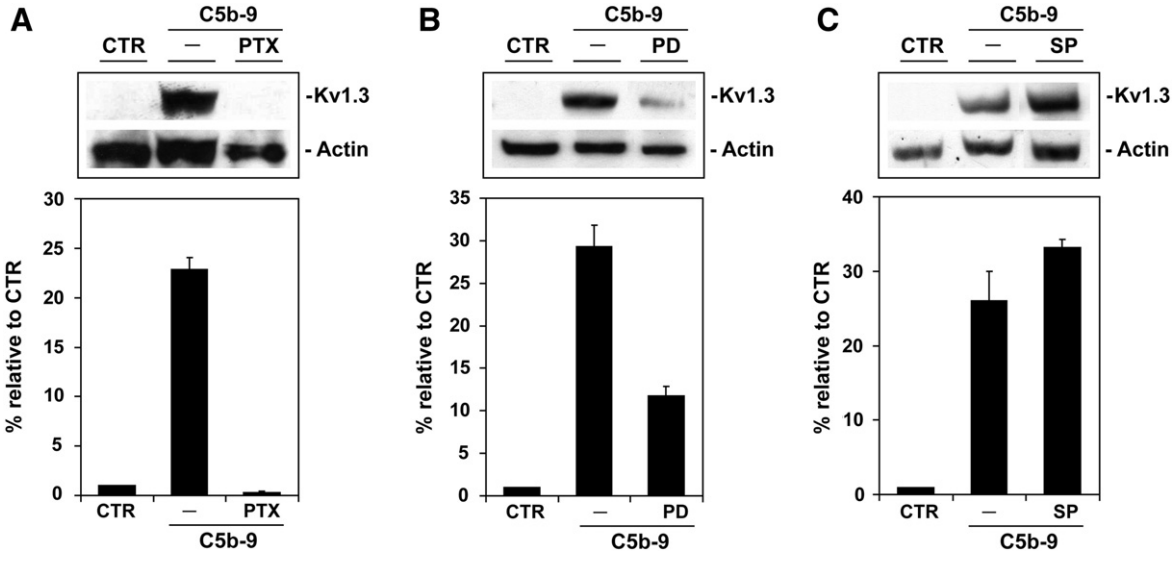

Fig. 5. $K_v1.3$ expression induced by C5b-9 is dependent on Gi protein and ERK activation. OLGs were pretreated with PTX (500 ng/ml) for 4 h or with PD98059 or SP600125 for 1 h, then exposed to C5b-9 for 30 min. Lysates were analyzed by western blotting for $K_v1.3$ and β-actin expression as described above. Exposure to PTX was able to reverse the effect of C5b-9 on $K_v1.3$ ($p = 0.032$) (A). A similar effect was seen when the MEK1 inhibitor PD98059 ($p = 0.05$) was used (B), but JNK inhibition by SP600125 (C) had no effect on $K_v1.3$ protein expression.

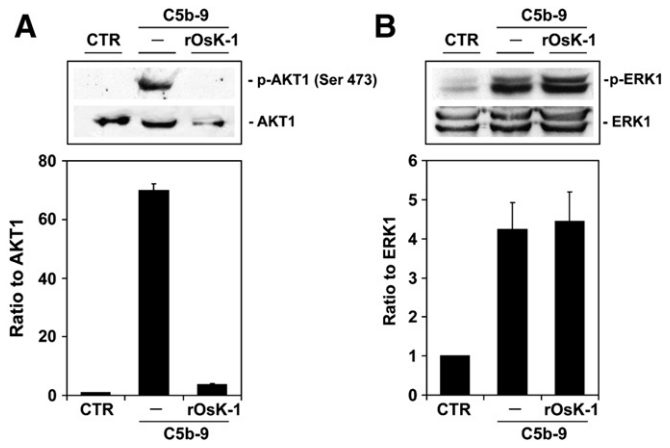

Fig. 6. Effect of rOsK-1 on the activation of Akt and ERK1. OLGs were cultured in defined medium and pretreated with rOsK-1 prior to stimulation with C5b-9. The effect of rOsK-1 on Akt (A) and ERK1 (B) phosphorylation was analyzed by western blotting. rOsK-1 was able to inhibit Akt phosphorylation ($p = 0.018$) but had no effect on ERK1 activation.

function of the up-regulated membrane currents, including $K_v1.3$-like currents, making them likely to be activated at voltages closer to the resting membrane potential; thus, less depolarization would be required to open the same channels in C5b-9-stimulated OLGs than in unstimulated OLGs.

Inhibition of sublytic C5b-9-induced expression of $K_v1.3$ and outward current by LY294002

To further investigate the mechanism of C5b-9-induced $K_v1.3$ protein expression in OLGs, we examined the signaling pathways that might be involved in its expression. Sublytic C5b-9 is able to activate both the PI3K and MAPK family pathways (Niculescu et al., 1999a; Soane et al., 2001). The C5b-9-induced expression of $K_v1.3$ was inhibited by LY294002 (20 μM), a specific PI3K inhibitor ($p = 0.016$) (Fig. 4A). To study the effect of LY294002 on outward current in OLGs pretreated with C5b-9, we performed electrophysiological measurements on 10 cells. Whole-cell currents were recorded from individual non-treated and C5b-9-treated cells before and after bath application of 20 μM LY294002. LY294002 blocked >90% of the total current and ~40% of the rapidly inactivating current (or types A) present after exposure to C5b-9 (Supplementary Fig. 2). The remaining currents were most probably $K_v1.4$ or $K_v4.2$, which are "A" type, fast and transient currents. Point-by-point subtraction of the current recorded after application of LY294002 (Supplementary Fig. 2C) from that recorded when the cell was treated with C5b-9 (Supplementary Fig. 2B) revealed the characteristics of current blocked by LY294002 (Fig. 4B). The blocked portion of the transient current was clearly visible in Fig. 4B (arrow). LY294002 also inhibited the phosphorylation of Akt (Fig. 4C) and its downstream substrate FOXO1 ($p = 0.006$) (Fig. 4D). These data indicate that LY294002 inhibits both the $K_v1.3$ protein and the current induced by C5b-9 and suggest that the activation of PI3K may be involved in $K_v1.3$ channel expression. It is important to mention that LY294002 has been shown to inhibit the outward K_v currents as well, by acting directly on the channel (El-Kholy et al., 2003).

Regulation of sublytic C5b-9-induced expression of $K_v1.3$

C5b-9 has been shown to induce PI3K and ERK1 through the activation of the Gi protein (Niculescu et al., 1999a; Soane et al., 2001). In our study, exposure of OLG to pertussis toxin (PTX), a Gi protein inhibitor, prior to stimulation with C5b-9 completely abolished the expression of $K_v1.3$ induced by C5b-9 ($p = 0.032$) (Fig. 5A). In addition, PD98059 (100 μM), a MEK1 inhibitor, also significantly reduced the expression of $K_v1.3$ ($p = 0.05$) (Fig. 5B). In contrast, SP 600125, a JNK inhibitor, had no effect on the C5b-9-induced expression of $K_v1.3$ (Fig. 5C). Thus, our data indicated that both the PI3K and ERK1 pathways are required for activation of $K_v1.3$ by C5b-9 and that activation of these pathways may be dependent on the activation of Gi proteins.

Akt as an intracellular target for $K_v1.3$

To further characterize the relationship between Akt and $K_v1.3$, we assessed the effect of inhibiting the expression of $K_v1.3$ on the Akt activation induced by C5b-9. Activation of Akt depends on the integrity of the pleckstrin homology domain, which mediates its membrane translocation, and on the phosphorylation of Thr308 in the activation loop and of Ser473 (Datta et al., 1999). To test the effect of the $K_v1.3$ inhibitor rOsk-1 on Akt activation, we examined the

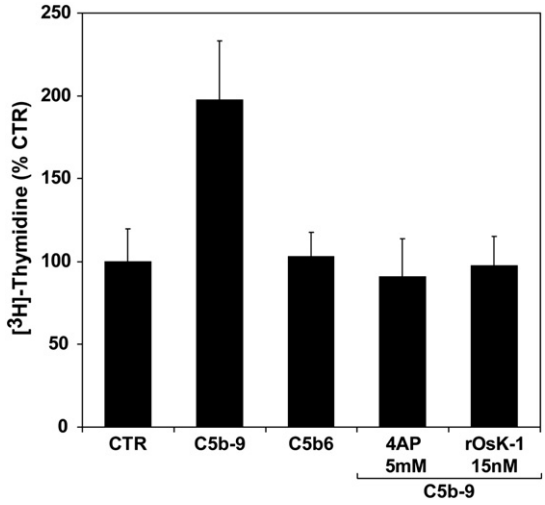

Fig. 7. Effect of $K_v1.3$ inhibition on DNA synthesis. OLGs were pretreated with rOsK-1 or 4AP for 1 h and then stimulated with serum C5b-9 for 24 h in the presence of 1 μCi [^{3}H] thymidine. C5b-9 significantly increased [^{3}H]thymidine incorporation when compared to C5b6 ($p = 0.005$). Both 4AP ($p = 0.001$) and rOsK-1 ($p = 0.003$) blocked the [^{3}H] thymidine incorporation induced by C5b-9. Three separate experiments were performed, and data are presented as means ± SEM.

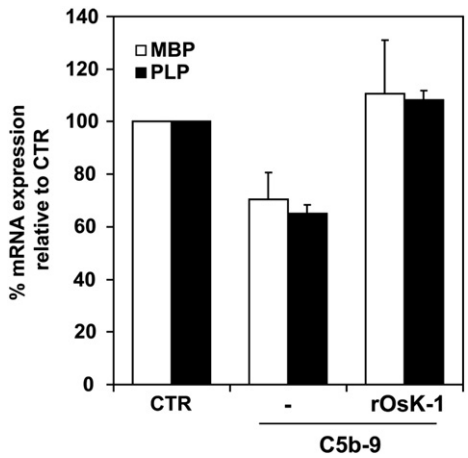

Fig. 8. Effect of rOsK-1 on C5b-9-induced down-regulation of MBP and PLP expression. OLGs were cultured in defined medium for 56 h, and then stimulated with C5b-9 for 6 h with or without rOsK-1 pretreatment. The expression of MBP and PLP mRNA was determined by real-time PCR. The expression of MBP and PLP decreased significantly after exposure to C5b-9 ($p = 0.05$ for MBP and $p = 0.004$ for PLP). Pretreatment with rOsK-1 abolished the down-regulation of MBP and PLP induced by C5b-9. Results of three separate experiments are expressed as mean ± SEM, relative to CTR (considered to be 100%).

phosphorylation of Akt at Ser 473. rOsk-1 was able to inhibit the C5b-9-induced phosphorylation of Akt at Ser 473 ($p = 0.018$) (Fig. 6A). Thus, our data indicated that activation of Akt is dependent on $K_v1.3$ channel activation. The fact that Akt activation was dependent on both PI3K and $K_v1.3$ indicates that Akt is situated downstream of both these signal transduction molecules. On the other hand, rOsK-1 had no effect on the C5b-9-induced activation of ERK1 (Fig. 6B), suggesting that the ERK1 is not affected by the activation of the $K_v1.3$ channels. Taken together, these data suggested that Akt might be one of the intracellular targets used by $K_v1.3$ channels to modulate cell cycle progression.

Reversal of C5b-9-induced cell cycle activation by inhibiting $K_v1.3$

The functional consequences of the $K_v1.3$ channel activation induced by C5b-9 in OLGs are currently unknown. We do know that C5b-9 induces cell cycle activation and that the PI3K pathway is important in this activation. Given this role for the PI3K pathway in $K_v1.3$ activation, we assessed the ability of $K_v1.3$ inhibitors to block the C5b-9-induced activation of the cell cycle in OLGs. We pretreated cells with rOsk-1, then stimulated them with C5b-9 and monitored DNA synthesis using [^{3}H]thymidine uptake as previously described (Rus et al., 1996). In the OLGs, C5b-9 induced a 2-fold increase in [^{3}H] thymidine incorporation when compared to C5b6-stimulated cells ($p = 0.005$). 4AP (5 mM, $p = 0.001$) and rOsK-1 5 nM ($p = 0.002$) and 15 nM ($p = 0.003$) were very effective in blocking the DNA synthesis induced by C5b-9 (Fig. 7). These data clearly indicated that $K_v1.3$ is required for the cell cycle activation induced by C5b-9 in OLGs.

Effect of $K_v1.3$ inhibition on MBP and PLP mRNA expression

Having shown that sublytic C5b-9 reduced the accumulation of mRNAs encoding MBP and PLP (Rus et al., 1996), we next investigated the effect of inhibiting $K_v1.3$ on the down-regulation of the myelin gene expression induced by C5b-9. As shown in Fig. 8, the down-regulation of MBP ($p = 0.05$) and PLP expression ($p = 0.004$) induced

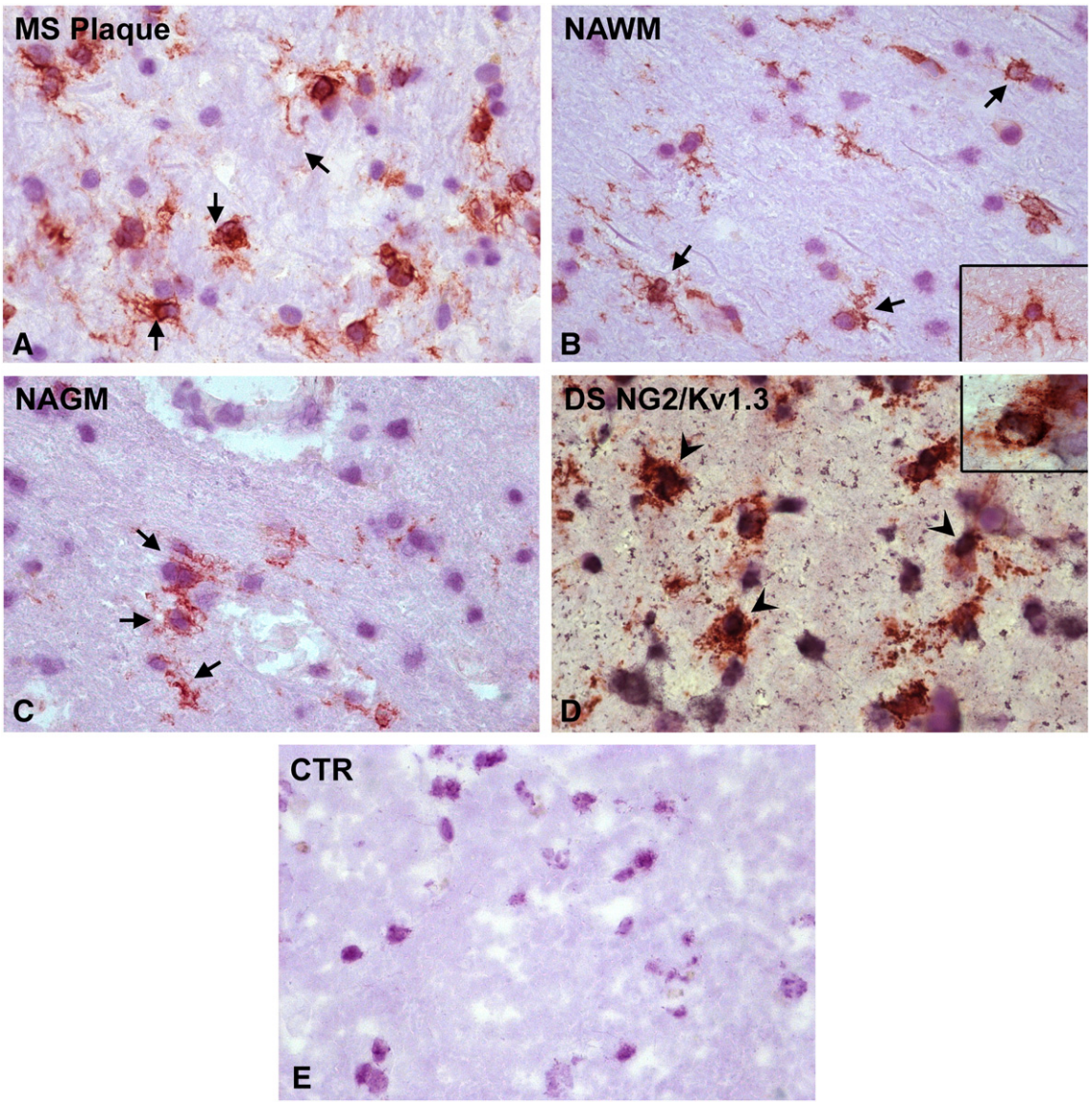

Fig. 9. Expression of NG2-positive cells in MS brain and colocalization with $K_v1.3$. Cryostat sections were immunostained for NG2 expression or double-stained for NG2 and $K_v1.3$. Expression of NG2 was abundant in MS active lesions, NAWM, and NAGM. $NG2^+$ cells in active MS plaques (A) and NAWM (B) displayed multibranched processes. A smaller number of $NG2^+$ cells were seen in the NAGM. These cells also appeared to have a lower number of multibranched processes (C). $NG2^+$ cells (red deposits) also expressed $K_v1.3$ (black deposits) (D). E. Control for the immunoperoxidase reaction. A–E: original magnification ×400. Inset: original magnification ×1000. (For interpretation of the references to color in this figure legend, the reader is referred to the web version of this article.)

Table 2
Expression of NG2, C5b-9 and Kv1.3 in MS brain.

Case no. (age, sex)	Lesion (no.)	Lesion type	NG2	C5b-9	Kv1.3
1	Frontal plaques (3)	Acute	++	++	+++
(38/F)		NAWM	ND	+	++
		NAGM	++	+	+
2	Occipital plaques (3)	Chronic active	++	++	++
(61/F)		NAWM	+	++	+
		NAGM	+	+	+
3	Parietal plaques (3)	Chronic active	++	++	++
(62/M)		NAWM	++	+++	++
		NAGM	++	ND	−
4	Frontal plaques (3)	Acute	++	ND	++
(51/F)		NAWM	ND	+	+
		NAGM	+	++	+
5	Frontal plaques (3)	Acute	+++	+/++	++
(61/F)		NAWM	++	+	++
		NAGM	++	+	++
6	Occipital plaques (3)	Acute	+	ND	++
(51,F)		NAWM	++	++	++
		NAGM	ND	+++	+

F, female; M, male; NAWM, normal appearing white matter; NAGM, normal appearing gray matter; −, negative; +, slightly positive; ++, positive; +++, highly positive; ND, not determined.

by serum C5b-9 was reversed by pretreatment of OLGs with rOsK-1. These data indicate the broader functional consequences of inhibiting $K_v1.3$ channel activation for the biological effects induced in OLGs by sublytic C5b-9.

$NG2^+$ cells express $K_v1.3$ and co-localized with C5b-9 in brains from MS patients

To identify putative OLG progenitor cells in the MS brain, we used immunohistochemical staining with a monoclonal antibody against NG2 chondroitin sulfate proteoglycan (Wilson et al., 2006). $NG2^+$ cells were found in active plaques as well as in NAWM and NAGM areas in brains of MS patients (Fig. 9, Table 2). The anti-NG2 antibody identified cells with several fine processes, and the expression of NG2 appeared to be higher in the brains of MS patients than in those of controls (data not shown). The NG2 deposits were rather extensive in some of the NAWM and NAGM areas (Figs. 9B,C). The pattern of staining was often both cytoplasmic and at the surface of the cell membrane (Fig. 9). Our data for NG2 staining in the MS brain were similar to those reported by Willson et al. (Wilson et al., 2006). The staining patterns that we observed for $K_v1.3$ indicated that it was expressed in both perivascular and parenchymal cells. As previously shown, some of the cells expressing $K_v1.3$ were CD3- and CD68-positive (Rus et al., 2005). By double staining, we found that most of the NG2-positive cells also expressed $K_v1.3$, suggesting that OPCs also express $K_v1.3$ in the MS brain (Fig. 9D).

The presence of C5b-9 deposits in MS brains was also investigated using an anti-C5b-9 neoantigens antibody (Niculescu et al., 2004). C5b-9 deposits were seen both at the cell surface and intracellularly. In addition to being present in MS plaques, C5b-9 deposits were found in NAWM and NAGM areas (Table 2, Figs. 10A,B), but the C5b-9 deposits in the NAWM and NAGM were less extensive than those in MS plaques. The extent of the C5b-9 deposits varied from one lesion to another (Table 2). On some serial sections, the pattern of NG2 staining was comparable to that of C5b-9. When we used a double-staining approach to further assess the pattern of C5b-9 deposits on $NG2^+$ cells, we found that some of the $NG2^+$ cells also had C5b-9 deposits (Fig. 10C). The NG2/C5b-9-positive cells were found in MS plaques as well as NAWM and NAGM areas. Controls of the immunoperoxidase reaction by excluding the primary antibody or by using isotype IgG were negative (Figs. 9E and 10D).

These data indicate that C5b-9 deposits in MS brains are present not only on macrophages, astrocytes, and OLGs, as previously reported

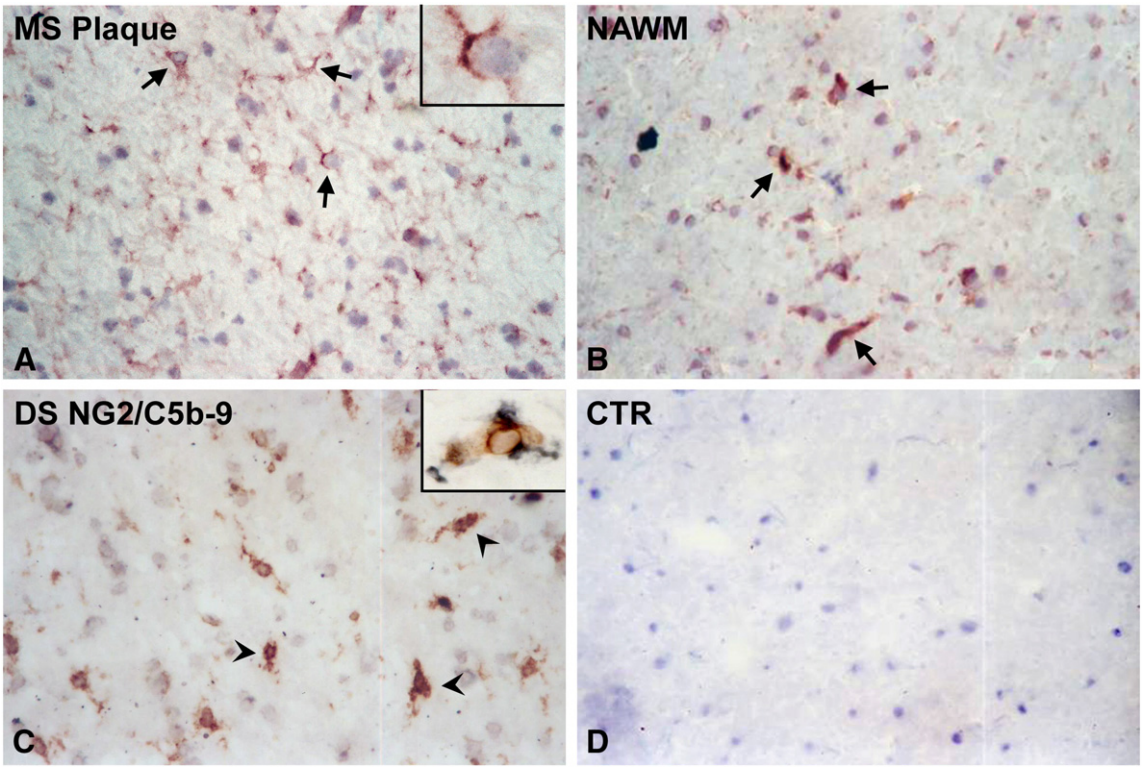

Fig. 10. C5b-9 deposits in MS brain and co-localization with NG2 cells. Cryostat sections of MS brain were stained for C5b-9 or double-stained for C5b-9 and NG2. C5b-9 deposits were found in active MS plaques (A) and NAWM (B). In double-staining analysis, $NG2^+$ cells (red deposits) also co-localized with C5b-9 deposits (black deposits) (arrowheads) (C). D. Control for the immunoperoxidase reaction. A–D: original magnification, ×400. Inset: original magnification, ×1000. (For interpretation of the references to color in this figure legend, the reader is referred to the web version of this article.)

(Barnett and Prineas, 2004; Breij et al., 2008; Compston et al., 1989; Storch et al., 1998), but also on NG2$^+$ OPCs. These data suggest that complement activation and C5b-9 assembly on OPCs may be an important modulator of K_v1.3 expression during demyelination in MS brains.

Discussion

Assembly of lytic C5b-9 induces cell death by necrosis or apoptosis (Nauta et al., 2002; Papadimitriou et al., 1994). In contrast, sublytic levels of C5b-9 promote cell survival and proliferation (Cudrici et al., 2006; Soane et al., 2001, 1999; Zwaka et al., 2003). The C5b-9 terminal complement complex, a hallmark of complement activation, is present in MS lesions (Breij et al., 2008; Lucchinetti et al., 2000) and is known to induce cell cycle activation in OLGs (Rus et al., 1997, 1996). In the present study, we examined the effect of sublytic C5b-9 on K_v1.3 potassium channel expression and its role in sublytic C5b-9-induced cell cycle activation in OLGs. We have shown for the first time that K_v1.3 channel activity is modulated by and necessary for C5b-9-induced cell cycle activation. Other K_v channels are presumably also influenced by C5b-9, because rOSk-1 had no effect on the currents generated after C5b-9 in some of the cells investigated. Our data suggest that, as a component of the macroscopic K_v current observed in OLGs, only a fraction of the K_v1.3 channels visualized by western blotting likely contribute to functional K_v current generation in the cell.

To investigate the mechanism of K_v1.3 protein up-regulation by C5b-9, we used cyclohexymide a protein synthesis inhibitor. The results of our pretreatment with cyclohexymide suggested that C5b-9 might stabilize K_v1.3 channel expression protein expression in the membrane, most probably by delaying normal degradation pathways (Colley et al., 2007). Moreover, the time course of the C5b-9 effect suggested that the hyperpolarizing shift in the voltage-dependence of K_v1.3 channel activation is supported by a functional modification, rather than by transcriptional changes (Niculescu et al., 1999b). Since different K_v1 subfamily members have different determinants for channel trafficking, further work will be required to identify additional mechanisms by which C5b-9 could increase the expression of K_v1.3. One might envision that C5b-9-induced signaling could serve to release K_v1.3 from the endoplasmic reticulum and thus delay the degradation of the channel from the plasma membrane during periods of activity aligned with C5b-9 signaling.

Our results point to an early involvement of K_v1.3 channels in the initial signaling events at the membrane level and also suggest a role for K_v1.3 channel modulation in C5b-9 mediated cell cycle signaling. We have shown for the first time that K_v1.3 is required in order for Akt to be activated by C5b-9 and mediate the cell cycle activation in OLGs. This role for K_v1.3 is consistent with the role of K_v channels in modulating the signaling mediated by other growth factors (Guo et al., 2005). Increases in K_v1.3 protein expression that occurred upon C5b-9 activation could be inhibited after exposure to the channel inhibitor rOsk-1, which blocks K_v1.3 channel activity. In addition, we found that rOsK-1 blocks K_v1.3 channel protein expression through a mechanism yet to be identified. This effect seems to be specific for channel protein expression, since rOsK-1 did not affect the expression of total Akt or β-actin.

In addition, we have shown that K_v1.3 plays a role in the dedifferentiation induced in OLGs by sublytic C5b-9 (Rus et al., 1996). The fact that K_v1.3 inhibition reverses the C5b-9 effect on MBP and PLP expression is important in view of the recent introduction of 4-AP extended-release tablets (dalfampridine) for the treatment of patients with MS (Bever and Judge, 2009; Goodman et al., 2009), suggesting that this therapy might have beneficial effects on OLG myelination in an inflammatory milieu.

To investigate this potential relationship in vivo, we examined the co-expression of NG2$^+$ cells and K_v1.3 and looked for co-localization with C5b-9 in the brains of MS patients. Our data indicated that most of the NG2$^+$ cells express K_v1.3 and that some of these cells also have C5b-9 deposits. All of these data suggest that our observed C5b-9 effects that we observed in vitro, including dedifferentiation and the effects on K_v1.3 expression may also occur in vivo in the brains of patients with MS. It is important to note that proliferating OLGs have been observed in vivo, in some active MS lesions (Solanky et al., 2001).

In conclusion, our results indicate that C5b-9 contributes to OLG survival by modulating the function of K_v1.3 channels, which play an important role in cell cycle activation by controlling Akt phosphorylation. This function of C5b-9 may have additional significance in situations in which cell cycle activation is induced in OLGs by C5b-9, in particular in experimental autoimmune encephalomyelitis and MS, conditions in which complement activation and C5b-9 assembly occur ubiquitously (Linington et al., 1989; Lucchinetti et al., 2000; Breij et al., 2008). Our data suggest that C5b-9 may promote the dedifferentiation and possibly prevent the differentiation of OPCs in vivo. Based on our findings, it is reasonable to speculate that inhibition of K_v1.3 expression could increase remyelination and differentiation of progenitor cells to OLGs in MS.

Supplementary materials related to this article can be found online at doi:10.1016/j.yexmp.2011.04.006.

Acknowledgments

We thank Dr. Deborah McClellan for editing this manuscript. This work was supported in part by the US Public Health Grant RO1 NS42011 (to H.R.) and a Veterans Administration Merit Award (to H.R.). MS brain tissues were obtained from Human Brain and Spinal Fluid Resource Center, Veterans Affairs West Los Angeles Health Care Center, CA USA, which is sponsored by the NINDS/NIH, NMSS and Dept. of Veterans Administration.

References

Attali, B., et al., 1997. Characterization of delayed rectifier Kv channels in oligodendrocytes and progenitor cells. J. Neurosci. 17, 8234–8245.
Bacia, A., et al., 2004. K+ channel blockade impairs remyelination in the cuprizone model. Glia 48, 156–165.
Barnett, M.H., Prineas, J.W., 2004. Relapsing and remitting multiple sclerosis: pathology of the newly forming lesion. Ann. Neurol. 55, 458–468.
Barres, B.A., Raff, M.C., 1999. Axonal control of oligodendrocyte development. J. Cell Biol. 147, 1123–1128.
Bever, C.T., Judge, S.I., 2009. Sustained-release fampridine for multiple sclerosis. Expert Opin. Investig. Drugs 18, 1013–1024.
Billon, N., et al., 2002. Normal timing of oligodendrocyte development depends on thyroid hormone receptor alpha 1 (TR{alpha}1). EMBO J. 21, 6452–6460.
Breij, E.C.W., Brink, B.P., Veerhuis, R., Van den Berg, C., Vloet, R., Yan, R., Dijkstra, C.D., Van der Valk, P., Bö, L., 2008. Homogeneity of active demyelinating lesions in established multiple sclerosis. Ann. Neurol. 63, 16–25.
Carney, D.F., et al., 1985. Elimination of terminal complement intermediates from the plasma membrane of nucleated cells: the rate of disappearance differs for cells carrying C5b-7 or C5b-8 or a mixture of C5b-8 with a limited number of C5b-9. J. Immunol. 134, 1804–1809.
Chittajallu, R., et al., 2002. Regulation of Kv1 subunit expression in oligodendrocyte progenitor cells and their role in G1/S phase progression of the cell cycle. Proc. Natl. Acad. Sci. U. S. A. 99, 2350–2355.
Colley, B.S., et al., 2007. Neurotrophin B receptor kinase increases Kv subfamily member 1.3 (Kv1.3) ion channel half-life and surface expression. Neuroscience 144, 531–546.
Compston, D.A., et al., 1989. Immunocytochemical localization of the terminal complement complex in multiple sclerosis. Neuropathol. Appl. Neurobiol. 15, 307–316.
Cragg, M.S., et al., 2000. Complement mediated cell death is associated with DNA fragmentation. Cell Death Differ. 7, 48–58.
Cudrici, C., et al., 2005. C5b-9 protects oligodendrocytes apoptosis by regulating BH-3-only proapoptotic proteins. FASEB J. 19, A324.
Cudrici, C., et al., 2006. C5b-9 terminal complex protects oligodendrocytes from apoptotic cell death by inhibiting caspase-8 processing and up-regulating FLIP. J. Immunol. 176, 3173–3180.
Cudrici, C., et al., 2008. Complement C5 regulates the expression of insulin-like growth factor binding proteins in chronic experimental allergic encephalomyelitis. J. Neuroimmunol. 203, 94–103.
Datta, S.R., et al., 1999. Cellular survival: a play in three Akts. Genes Dev. 13, 2905–2927.

El-Kholy, W., et al., 2003. The phosphatidylinositol 3-kinase inhibitor LY294002 potently blocks K(V) currents via a direct mechanism. FASEB J. 17, 720–722.
Fosbrink, M., et al., 2009. Response gene to complement 32 is required for C5b-9 induced cell cycle activation in endothelial cells. Exp. Mol. Pathol. 86, 87–94.
Ghiani, C.A., et al., 1999. Voltage-activated K+ channels and membrane depolarization regulate accumulation of the cyclin-dependent kinase inhibitors p27(Kip1) and p21(CIP1) in glial progenitor cells. J. Neurosci. 19, 5380–5392.
Goodman, A.D., et al., 2009. Sustained-release oral fampridine in multiple sclerosis: a randomised, double-blind, controlled trial. Lancet 373, 732–738.
Guo, T.B., et al., 2005. Insulin-activated, K+−channel-sensitive Akt pathway is primary mediator of ML-1 cell proliferation. Am. J. Physiol. Cell Physiol. 289, C257–C263.
Linington, C., et al., 1989. Immunohistochemical localisation of terminal complement component C9 in experimental allergic encephalomyelitis. Acta Neuropathol. (Berl.) 79, 78–85.
Lucchinetti, C., et al., 2000. Heterogeneity of multiple sclerosis lesions: implications for the pathogenesis of demyelination. Ann. Neurol. 47, 707–717.
Nauta, A.J., et al., 2002. The membrane attack complex of complement induces caspase activation and apoptosis. Eur. J. Immunol. 32, 783–792.
Niculescu, F., et al., 1997. Activation of Ras and mitogen-activated protein kinase pathway by terminal complement complexes is G protein dependent. J. Immunol. 158, 4405–4412.
Niculescu, F., et al., 1999a. Sublytic C5b-9 induces proliferation of human aortic smooth muscle cells: role of mitogen activated protein kinase and phosphatidylinositol 3-kinase. Atherosclerosis 142, 47–56.
Niculescu, F., et al., 1999b. Tyrosine phosphorylation and activation of Janus kinase 1 and STAT3 by sublytic C5b-9 complement complex in aortic endothelial cells. Immunopharmacology 42, 187–193.
Niculescu, F., et al., 2004. C5b-9 terminal complement complex assembly on apoptotic cells in human arterial wall with atherosclerosis. Exp. Mol. Pathol. 76, 17–23.
Papadimitriou, J.C., et al., 1991. Quantitative analysis of adenine nucleotides during the prelytic phase of cell death mediated by C5b-9. J. Immunol. 147, 212–217.
Papadimitriou, J.C., et al., 1994. Ultrastructural studies of complement mediated cell death: a biological reaction model to plasma membrane injury. Virchows Arch. 424, 677–685.
Rus, H.G., et al., 1996. Sublytic complement attack induces cell cycle in oligodendrocytes. J. Immunol. 156, 4892–4900.
Rus, H., et al., 1997. Terminal complement complexes induce cell cycle entry in oligodendrocytes through mitogen activated protein kinase pathway. Immunopharmacology 38, 177–187.
Rus, H., et al., 2005. The voltage-gated potassium channel Kv1.3 is highly expressed on inflammatory infiltrates in multiple sclerosis brain. Proc. Natl. Acad. Sci. U. S. A. 102, 11094–11099.
Rus, H., et al., 2006. The complement system in central nervous system diseases. Autoimmunity 39, 395–402.
Scolding, N.J., et al., 1989. Vesicular removal by oligodendrocytes of membrane attack complexes formed by activated complement. Nature 339, 620–622.
Soane, L., et al., 1999. Inhibition of oligodendrocyte apoptosis by sublytic C5b-9 is associated with enhanced synthesis of bcl-2 and mediated by inhibition of caspase-3 activation. J. Immunol. 163, 6132–6138.
Soane, L., et al., 2001. C5b-9 terminal complement complex protects oligodendrocytes from death by regulating Bad through phosphatidylinositol 3-kinase/Akt pathway. J. Immunol. 167, 2305–2311.
Solanky, M., et al., 2001. Proliferating oligodendrocytes are present in both active and chronic inactive multiple sclerosis plaques. J. Neurosci. Res. 65, 308–317.
Soliven, B., et al., 1989. Expression and modulation of K+ currents in oligodendrocytes: possible role in myelinogenesis. Dev. Neurosci. 11, 118–131.
Storch, M.K., et al., 1998. Multiple sclerosis: in situ evidence for antibody- and complement-mediated demyelination. Ann. Neurol. 43, 465–471.
Tang, D.G., et al., 2001. Lack of replicative senescence in cultured rat oligodendrocyte precursor cells. Science 291, 868–871.
Trapp, B.D., et al., 1997. Differentiation and death of premyelinating oligodendrocytes in developing rodent brain. J. Cell Biol. 137, 459–468.
Vautier, F., Belachew, S., Chittajallu, R., Gallo, V., 2004. Shaker-type potassium channel subunits differentially control oligodendrocyte progenitor proliferation. Glia 48, 337–345.
Wilson, H.C., et al., 2006. Co-expression of PDGF alpha receptor and NG2 by oligodendrocyte precursors in human CNS and multiple sclerosis lesions. J. Neuroimmunol. 176, 162–173.
Zwaka, T.P., et al., 2003. The terminal complement complex inhibits apoptosis in vascular smooth muscle cells by activating an autocrine IGF-1 loop. FASEB J. 17, 1346–1348.